

## MICROSTRUCTURE OF THE PLASMA SPRAYED NiCrAlY COATING ISOTHERMALLY EXPOSED AT 850 °C FOR 6 MINUTES

KAROL IŽDINSKÝ, JOZEF IVAN, MILINA ZEMÁNKOVÁ

Results of structural studies performed with light microscopy and transmission electron microscopy on plasma sprayed NiCrAlY coating isothermally exposed at 850 °C for 6 minutes are presented in this paper. The applied thermal treatment led to the decomposition of initial phases and to precipitation of  $\alpha$ -Cr and  $\gamma'$ -Ni<sub>3</sub>Al. It is shown that the precipitation of  $\alpha$ -Cr and  $\gamma'$ -Ni<sub>3</sub>Al as well as the decomposition of martensitic NiAl obeyed orientation relationships. Dissolution of Ni<sub>5</sub>Y yttride was not observed. All the oxide inclusions remained amorphous and their transformation into crystalline structures is expected after longer exposures at 850 °C or at higher exposure temperatures.

## MIKROŠTRUKTÚRA PLAZMOVÉHO POVLAKU TYPU NiCrAlY PO 6-MINÚTOVEJ IZOTERMICKEJ EXPOZÍCII PRI TEPLOTE 850 °C

V práci sú uvedené výsledky štúdia štruktúry plazmového povlaku typu NiCrAlY po 6-minútovej izotermickej expozícii pri teplote 850 °C. Výsledky získané pomocou svetelnej mikroskopie a transmisnej elektrónovej mikroskopie ukázali, že uvedené tepelné spracovanie viedlo k rozpadu pôvodnej štruktúry nástreku a k precipitácii  $\alpha$ -Cr a  $\gamma'$ -Ni<sub>3</sub>Al. V práci je ukázané, že precipitácia  $\alpha$ -Cr a  $\gamma'$ -Ni<sub>3</sub>Al, rovnako ako aj rozpad martenzitickéj fázy NiAl sa riadia orientačnými vzťahmi. Rozpúšťanie ytridu Ni<sub>5</sub>Y nebolo pozorované. Všetky oxidové vtrúseniny ostali amorfné a ich transformáciu na kryštalické oxidy možno očakávať pri dlhších expozičných časoch alebo pri vyššej teplote expozície.

Key words: NiCrAlY coating, microstructure, thermal treatment, TEM studies

### 1. Introduction

AMDRY 962 – an alloy nickel base powder (NiCrAlY) is used for protective plasma spray coatings in hot corrosive or oxidising environments at high temperatures. It can also be used as hot corrosion and oxidation resistant bond coat

Ing. K. Iždinský, CSc., Ing. J. Ivan, CSc., RNDr. M. Zemánková, Ústav materiálov a mechaniky strojov SAV, Račianska 75, 838 12 Bratislava 38, SR.

for thermal barrier zirconia coatings. Our previous studies performed on NiCrAlY coating plasma sprayed in air [1] have shown that the coating is formed by a heterogeneous mixture of matrix metal, non-molten powders and oxide inclusions. The structure of the matrix metal with the hardness of 223 HV10 is fine-grained with the grain sizes not exceeding  $1\ \mu\text{m}$ . It was found to consist of nickel-based solid solution  $\gamma$ -Ni with bcc structure, martensitic NiAl with a tetragonal  $L1_0$  structure and  $\beta$ -NiAl with B2 crystal structure. Y is predominantly bound in the  $\text{Ni}_5\text{Y}$  yttride located in the grain boundary regions. Oxide inclusions are mostly aluminium base oxides with different amounts of Y, Cr or Ni. Chromium base oxides were rarely observed, too. All the oxide inclusions with no respect to their composition were determined as amorphous structures. As the heterogeneous structure of the coating is far from the equilibrium state that would be a welcome precondition for service at higher temperatures, the importance of the knowledge of the effect of thermal treatment on the structure of the coating appeared. The aim of this work is to present results obtained by structural studies performed on short time isothermally exposed plasma sprayed NiCrAlY coating at the temperature of  $850^\circ\text{C}$ .

## 2. Experimental material and procedure

Nickel base powder AMDRY 962, with a nominal composition Ni22Cr10Al1.0Y and sizes ranging from 106 to  $45\ \mu\text{m}$ , was plasma sprayed onto a steel substrate at a total power input of 32 kW. The coating was removed from the substrate and further isothermally exposed at  $850^\circ\text{C}$  for 6 minutes. The heating rate was  $20^\circ\text{C}/\text{minute}$  and subsequent cooling of samples was performed in air.

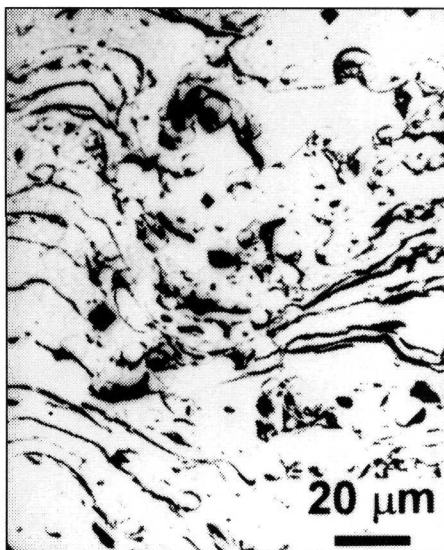
The same plasma spraying procedure as well as analytical equipment and techniques including light microscopy (LM) and transmission electron microscopy (TEM), as reported in previous studies [1–4], were used also in the present work and so the details will not be repeated here.

## 3. Results

The light microscopy observations revealed that the coating is formed by a heterogeneous mixture of light matrix metal and numerous darkly appearing oxide inclusions. Structure in the cross-section of the coating with respect to the substrate surface is shown in Fig. 1. The inclusions known from previous studies [1] are of various, mostly elongated shapes. The matrix metal displays a relatively homogeneous structure. The typical casting structure of particles that had not been melted in the plasma beam was not observed. Vickers hardness measurements showed that the average hardness of the coating was 384 HV10.

The microstructure of the coating was further characterised by the TEM. Both phase composition as well as morphology have changed when compared with the as-plasma sprayed microstructure [1].

Fig. 1. Light micrograph of the cross-section of thermally treated NiCrAlY coating (ion etched).



Precipitates with elongated shapes appeared in the structure of the coating. These precipitates are of different lengths as it can be seen in Figs. 2 and 3. They were mostly found in the  $\gamma/\gamma'$  grains and have been identified by selected area electron diffraction (SAED) as solid solution  $\alpha$ -Cr base phase. In some regions the  $\alpha$ -Cr precipitates displayed the morphology of a newly formed coherent phase obeying an orientation relationship to the matrix grain as it can be seen in Fig. 2. In other locations the  $\alpha$ -Cr precipitates appeared as relatively well developed non-coherent phase as shown in Fig. 3.

Matrix of the coating is formed by the nickel-based solid solution  $\gamma$ -Ni with coherent precipitates of  $\gamma'$ -Ni<sub>3</sub>Al. This is confirmed by the presence of forbidden reflections in the SAED patterns corresponding to  $\gamma$ -Ni. The precipitates of  $\gamma'$ -Ni<sub>3</sub>Al are too small to give enough contrast and therefore their observation is difficult and their morphology can be hardly determined. A typical example is shown in Fig. 4, where  $\gamma'$ -Ni<sub>3</sub>Al precipitates with not fully developed cuboidal morphology can be seen. These are separated by antiphase boundaries and thin regions of disordered  $\gamma$  as confirmed by TEM. No  $\beta$ -NiAl phase was observed in the microstructure of the thermally treated coating. In some regions the decomposition structure of martensitic NiAl and the newly formed  $\gamma/\gamma'$  phase were observed. A typical example is shown in Fig. 5. The formation of  $\gamma/\gamma'$  obeyed an orientation relationship shown in the indexed schematic in Fig. 5c.

Y, known from previous works to be bound besides oxide inclusions predominantly in the Ni<sub>5</sub>Y yttride, could have been found again in the grain boundary

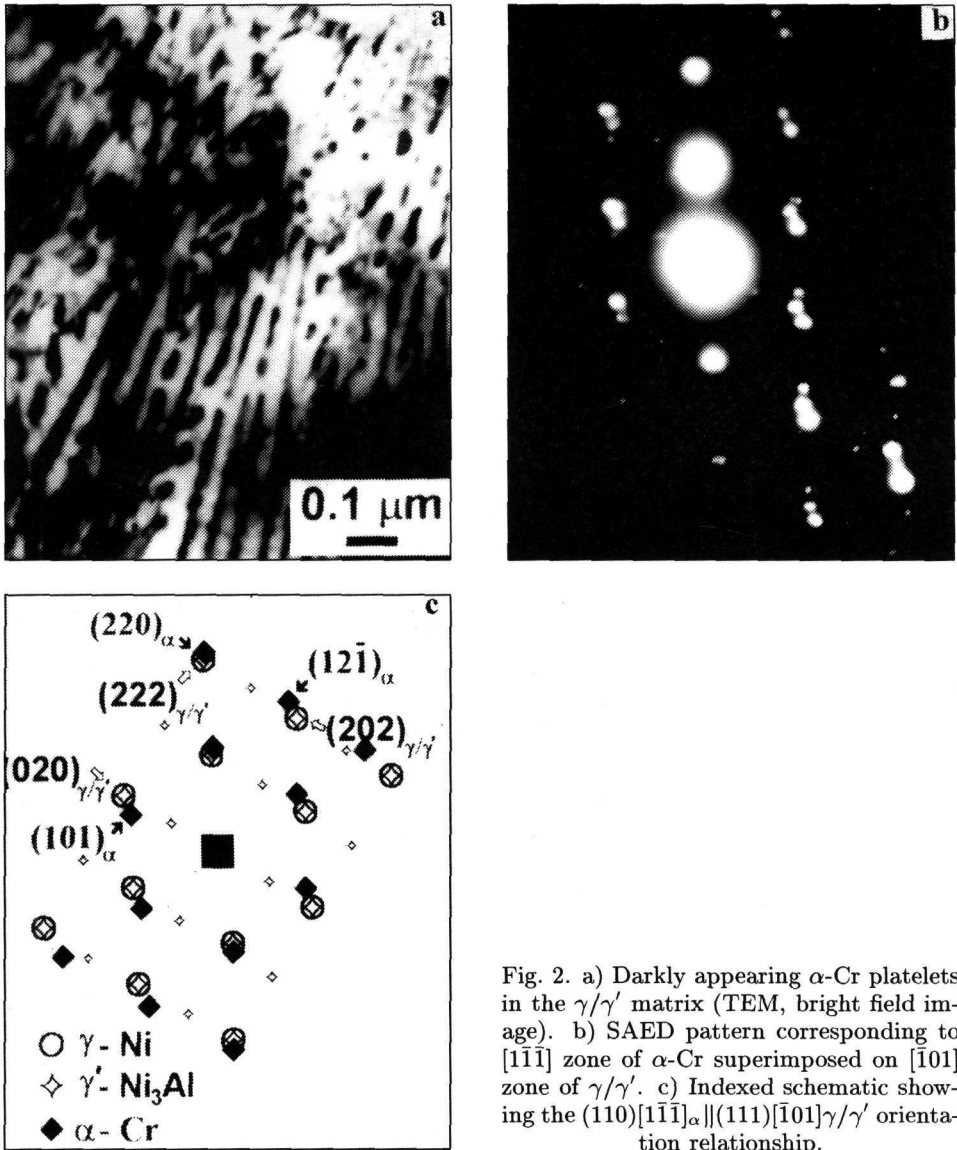


Fig. 2. a) Darkly appearing  $\alpha$ -Cr platelets in the  $\gamma/\gamma'$  matrix (TEM, bright field image). b) SAED pattern corresponding to  $[\bar{1}\bar{1}\bar{1}]$  zone of  $\alpha$ -Cr superimposed on  $[\bar{1}01]$  zone of  $\gamma/\gamma'$ . c) Indexed schematic showing the  $(110)[\bar{1}\bar{1}\bar{1}]_{\alpha} \parallel (111)[\bar{1}01]_{\gamma/\gamma'}$  orientation relationship.

regions as Ni<sub>5</sub>Y yttride. A typical example is shown in Fig. 6.

The amorphous oxide inclusions represent the last thermodynamically non-equilibrium phase in the microstructure of the coating. Observations by the TEM confirmed that all the oxide inclusions remain amorphous even after the applied 6-minute exposure at 850 °C. A typical example with nickel-based solid solution  $\gamma$ -Ni grains close to the spherical amorphous oxide inclusion is shown in Fig. 7.

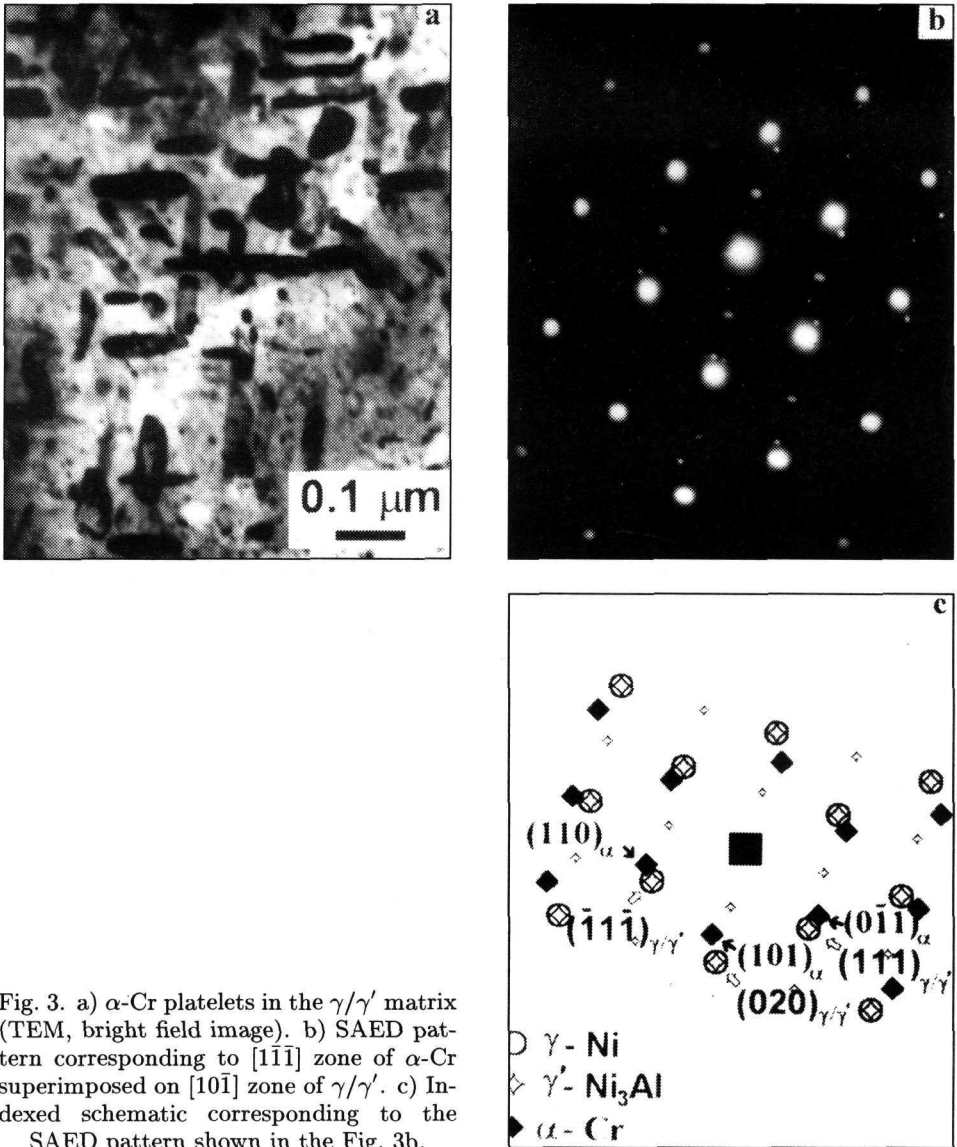


Fig. 3. a)  $\alpha$ -Cr platelets in the  $\gamma/\gamma'$  matrix (TEM, bright field image). b) SAED pattern corresponding to  $[1\bar{1}\bar{1}]$  zone of  $\alpha$ -Cr superimposed on  $[10\bar{1}]$  zone of  $\gamma/\gamma'$ . c) Indexed schematic corresponding to the SAED pattern shown in the Fig. 3b.

However, it should be noted that the  $\gamma$ -Ni grains were determined in the structure of the coating only quite exceptionally.

#### 4. Discussion of results

Already the light microscopy observations indicated that the applied thermal treatment had resulted in the important changes in the structure of the coating.

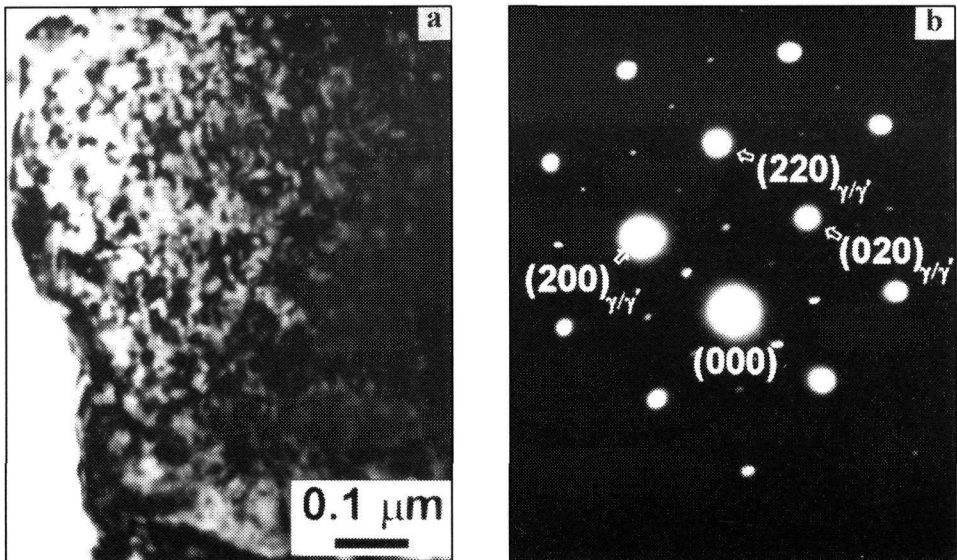


Fig. 4. a)  $\gamma/\gamma'$  grain with  $\gamma'$ - $\text{Ni}_3\text{Al}$  cuboids separated by both antiphase boundaries and thin regions of disordered  $\gamma$ -Ni (TEM, bright field image). b) SAED pattern corresponding to  $[001]$  zone of  $\gamma/\gamma'$ .

This is confirmed above all by the fact that the casting structure of the non-molten particles disappeared in the as-plasma sprayed structure formed by  $\gamma$ -Ni, martensitic NiAl and  $\beta$ -NiAl phases. It was replaced by a relatively homogeneous structure of the light matrix metal. The hardness of 384 HV<sub>10</sub> of the thermally treated coating is approximately of 72 % higher than the hardness of as-plasma sprayed coating (223 HV<sub>10</sub>). This is undoubtedly due to the phase transformations initiated by the applied thermal treatment. The TEM observations fully confirmed these assumptions. It appeared that the decomposition of non-equilibrium as-plasma sprayed microstructure took place and new phases were formed. The platelet precipitates determined as  $\alpha$ -Cr represent the dominant characteristic feature of the structure. Orientation relationship between  $\alpha$ -Cr and  $\gamma/\gamma'$  as shown in Fig. 2c and its variants were often observed in the initial stages of precipitation. This orientation relationship is based on the close interplanar distances of (110) of  $\alpha$ -Cr, where  $d_{(110)} = 0.2036$  nm, and (111) of  $\gamma/\gamma'$ , where  $d_{(111)} = 0.2031$  nm. However, this orientation relationship is no more obeyed by large  $\alpha$ -Cr precipitates exhibiting the loss of coherency with the matrix metal as shown in Fig. 3.

The precipitation of  $\alpha$ -Cr phase is accompanied or preceded by the formation of coherent  $\gamma'$ - $\text{Ni}_3\text{Al}$ . Both are equilibrium phases at temperatures below 1000 °C

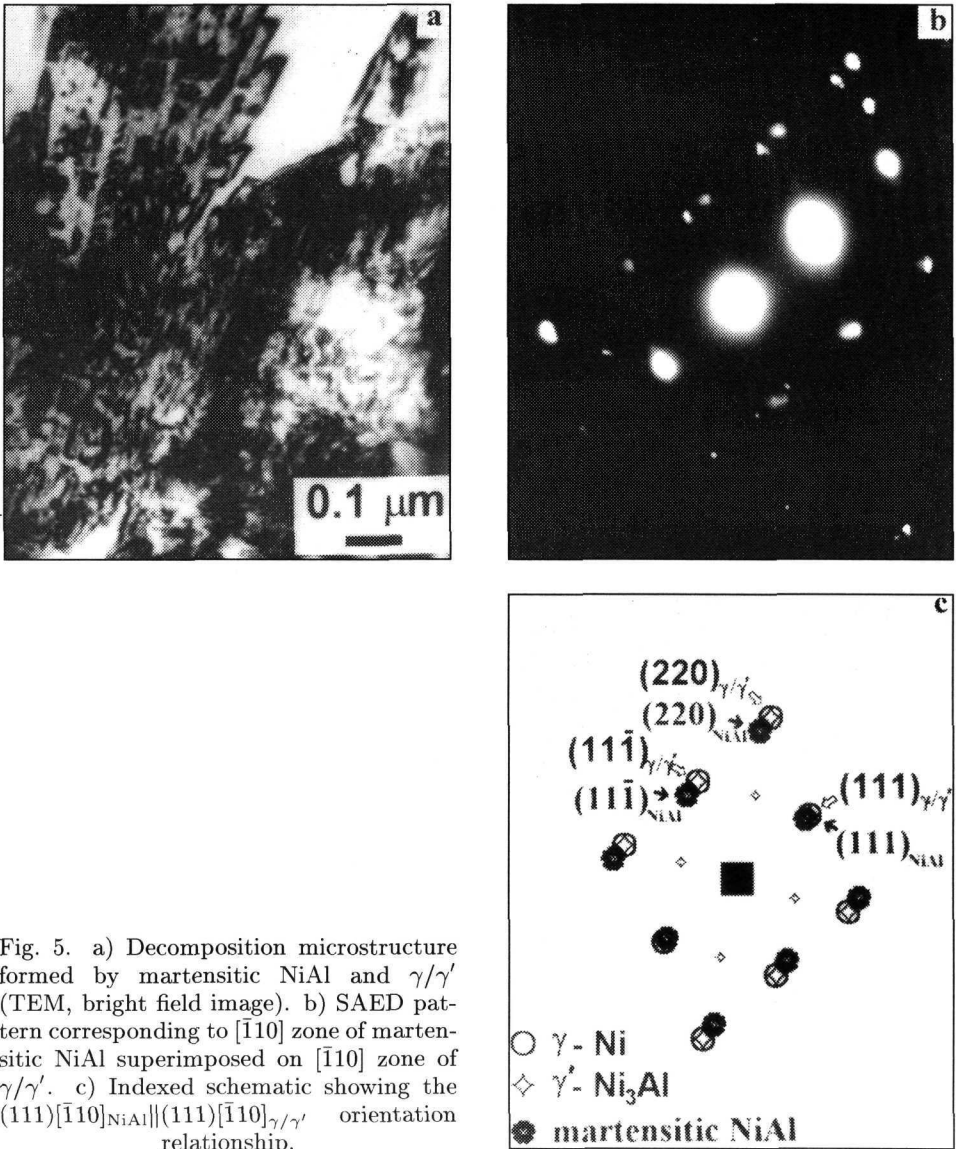


Fig. 5. a) Decomposition microstructure formed by martensitic NiAl and  $\gamma/\gamma'$  (TEM, bright field image). b) SAED pattern corresponding to  $[\bar{1}10]$  zone of martensitic NiAl superimposed on  $[\bar{1}10]$  zone of  $\gamma/\gamma'$ . c) Indexed schematic showing the  $(111)[\bar{1}10]_{\text{NiAl}} \parallel (111)[\bar{1}10]_{\gamma/\gamma'}$  orientation relationship.

in the NiCrAl system, and both are decomposition products of  $\gamma$ -Ni and  $\beta$ -NiAl [5]. Due to the inhomogeneity of initial microstructure these transformations can hardly be described in detail. Their sequence is undoubtedly governed by the local chemistry. According to the results of authors [5] the transformation begins with the precipitation of  $\gamma'$ -Ni<sub>3</sub>Al followed by the  $\alpha$ -Cr. However, there were no martensitic NiAl in the microstructure they had studied. The precipitation of  $\gamma'$ -

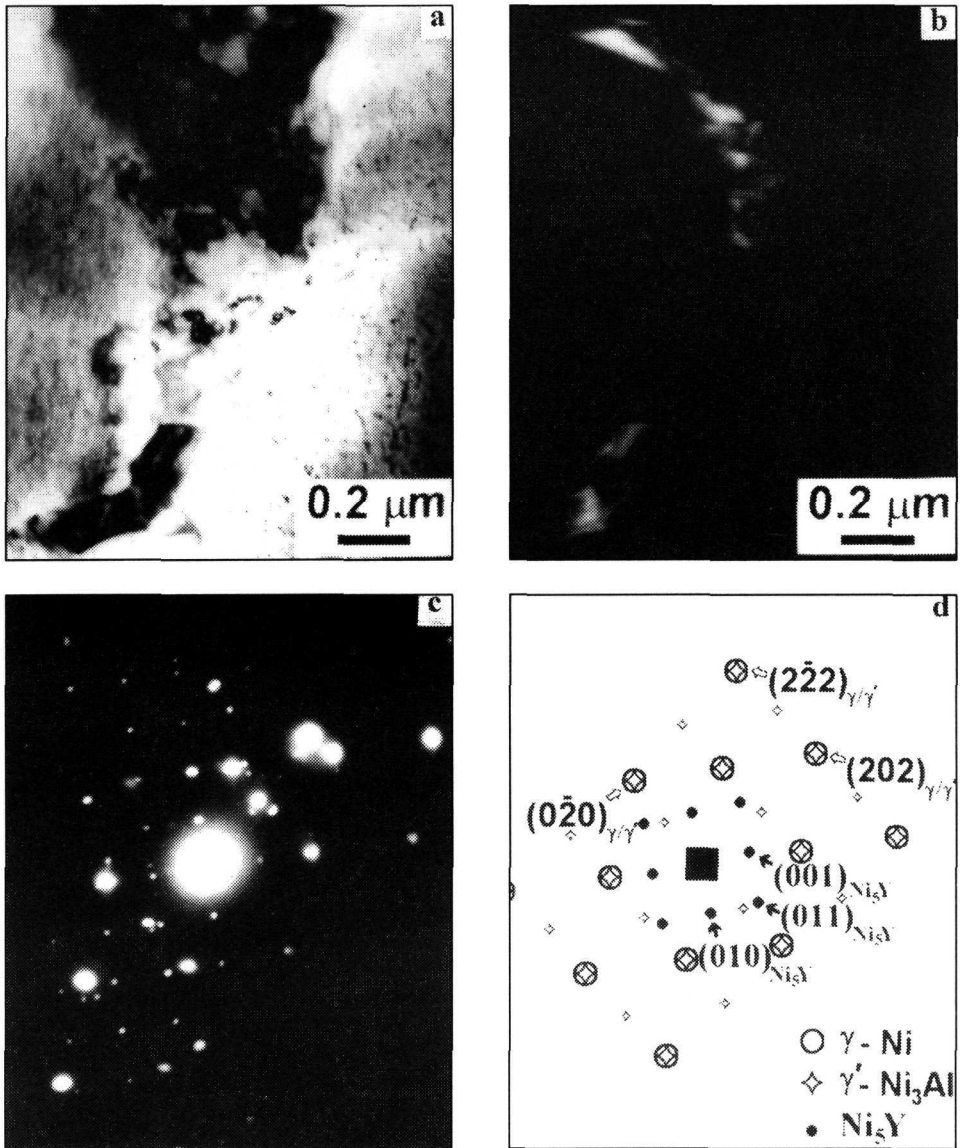


Fig. 6. a)  $\text{Ni}_5\text{Y}$  yttride in the grain boundary regions of  $\gamma/\gamma'$  (TEM, bright field image). b) Dark field image formed using the (001) reflection of  $\text{Ni}_5\text{Y}$ . c) SAED pattern corresponding to the [100] zone of  $\text{Ni}_5\text{Y}$  superimposed on  $[10\bar{1}]$  zone of  $\gamma/\gamma'$ . d) Indexed schematic corresponding to the SAED pattern shown in the Fig. 6c.



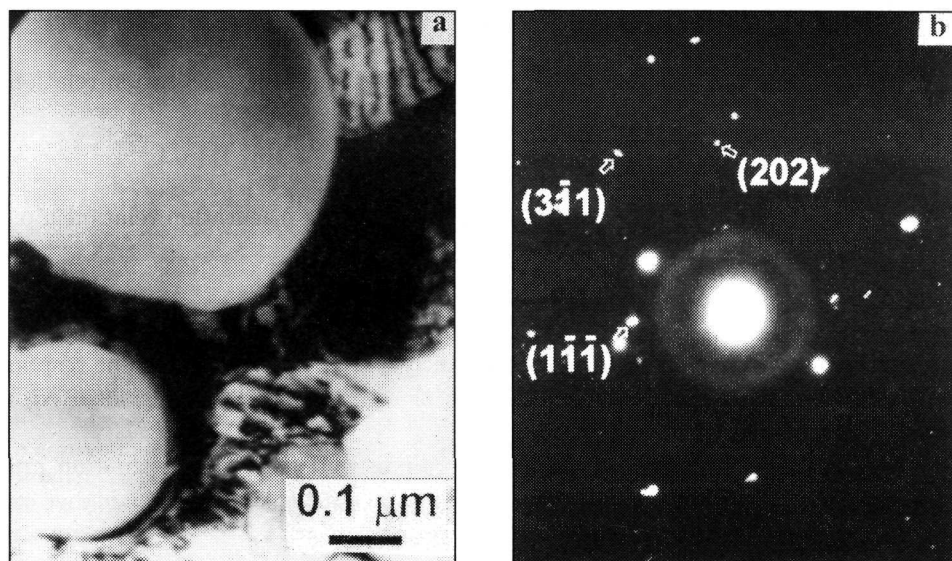


Fig. 7. a) Spherical amorphous oxide inclusions in the microstructure of thermally treated NiCrAlY coating (TEM, bright field image). b) SAED patterns showing the  $[12\bar{1}]$  zone  $\gamma$ -Ni diffraction spots and the diffuse scattering corresponding to amorphous oxide phase.

$\gamma$ -Ni<sub>3</sub>Al in the microstructure of martensitic NiAl was shown in the present work. This transformation can be again described by an orientation relationship based on the close interplanar distances of (111) of martensitic NiAl, where  $d_{(111)} = 0.2069$  nm, and (111) of  $\gamma/\gamma'$ , where  $d_{(111)} = 0.2031$  nm. The precipitation of coherent phases, predominantly  $\gamma'$ -Ni<sub>3</sub>Al, can well explain the dramatic increase in the hardness of the thermally treated coating.

TEM observations further confirmed the presence of Ni<sub>5</sub>Y yttride what means that the dissolution of this intermetallic phase did not take place within the applied thermal treatment. This is in accordance with the results presented by the authors [6].

Finally the transformation of amorphous oxides into crystalline structures was expected but not confirmed. All the oxide inclusions remained amorphous and their transformation is to be expected after longer exposures at 850°C or at higher exposure temperatures.

## 5. Conclusions

The microstructure of NiCrAlY (AMDRY 962) plasma sprayed coating isothermally exposed at the temperature 850°C for 6 minutes was studied in this paper.

The thermal treatment led to the decomposition of initial phases and to precipitation of  $\alpha$ -Cr and  $\gamma'$ -Ni<sub>3</sub>Al.

Precipitation of  $\alpha$ -Cr and  $\gamma'$ -Ni<sub>3</sub>Al obeyed the following orientation relationship:

$$(110)[\bar{1}\bar{1}\bar{1}]_{\alpha} \parallel (111)[\bar{1}01]_{\gamma/\gamma'}$$

Decomposition of martensitic NiAl obeyed the following orientation relationship:

$$(111)[\bar{1}10]_{\text{NiAl}} \parallel (111)[\bar{1}10]_{\gamma/\gamma'}$$

Precipitation of coherent phases, predominantly  $\gamma'$ -Ni<sub>3</sub>Al, was found to be responsible for the dramatic increase of hardness of the coating. Dissolution of Ni<sub>5</sub>Y yttride was not observed.

All the oxide inclusions remained amorphous and their transformation into crystalline structures is expected after longer exposures at 850°C or at higher exposure temperatures.

### Acknowledgements

The authors gratefully acknowledge the Scientific Grant Agency of the Ministry of Education of the Slovak Republic and Slovak Academy of Sciences (Grant project No. 5096/98) for the financial support of this work, and Mr. V. Kolenčiak for the preparation of plasma sprayed samples.

### REFERENCES

- [1] IŽDINSKÝ, K.—IVAN, J.—ZEMÁNKOVÁ, M.—KOLENČIAK, V.: *Kovove Mater.*, 36, 1998, p. 367.
- [2] IŽDINSKÝ, K.—IVAN, J.—ZEMÁNKOVÁ, M.—KOLENČIAK, V.: *Kovove Mater.*, 35, 1997, p. 188.
- [3] IŽDINSKÝ, K.—IVAN, J.—ZEMÁNKOVÁ, M.—KOLENČIAK, V.: *Kovove Mater.*, 35, 1997, p. 322.
- [4] IŽDINSKÝ, K.—IVAN, J.—ZEMÁNKOVÁ, M.—KOLENČIAK, V.: *Kovove Mater.*, 36, 1998, p. 87.
- [5] KUPČENKO, G. V.—NESTEROVIČ, L. N.: *Struktura i svojstva evtektičeskich kompozicionnykh materialov*. Minsk, Nauka i tehnika 1986.
- [6] SACRÉ, S.—WIENSTROTH, U.—FELLER, G.—THOMAS, L. K.: *Journal of Materials Science*, 28, 1993, p. 1843.